BEAM DYNAMICS IN LINAC4 AT CERN

A.M. Lombardi, G. Bellodi, M. Eshraqi, F. Gerigk, J.-B. Lallement, S. Lanzone, E. Sargsyan,
CERN, Geneva, Switzerland
R. Duperrier, D. Uriot, CEA, Saclay, France.

Abstract

Linac4 [1] is a linear accelerator for negative Hydrogen ions (H−), which will replace the 50 MeV proton Linac (Linac2) as linear injector for the CERN accelerators. The higher output energy (160 MeV) together with charge-exchange injection will allow increasing beam intensity in the following machines. Linac4 is about 100m long, normal-conducting, and will be housed in a tunnel 12m below ground on the CERN Meyrin site. The location has been chosen to allow using Linac4 as the first stage of acceleration for a Multi-MegaWatt superconducting Linac (SPL [2]).

End-to-end beam dynamics simulations have been carried out in parallel with the codes PATH [3] and TRACEWIN [4]. Following the definition of the layout, statistical studies have been carried out in order to define the alignment tolerances and correction system that guarantee a radiologically safe operation at the highest beam duty cycle as well as the maximum level of RF phase and amplitude jitter the system can tolerate before beam quality at injection in the PS Booster - and later in the SPL- is compromised

INTRODUCTION

Linac4 is a new Linac to be built at CERN within the framework of the proton injector's upgrade activities approved by the CERN council in June07. Initially Linac4 is meant to substitute the present CERN proton Linac, Linac2 which has provided protons to the PS booster since 1978. The beam peak current and the duty cycle for the first stage of operation are 80 mA and 0.1% respectively, making the design of Linac4 challenging for the control of space charge effects on beam quality, but not extremely challenging for the control of beam losses, due to the relatively low average current. Linac4 is also meant to serve as a front-end for a high power Superconducting Linac (the SPL) which is designed to work with the same peak current but a higher duty cycle, up to 6%. The beam dynamics studies reported in the following aim to predict beam quality and beam losses for the two different modes of operation.

LAYOUT

Linac4 is a normal conducting linear accelerator operating at the frequency of 352MHz. The first element of Linac4 is a RF volume source which provides a 400 microsec 80 mA H- beam at 45 keV with a repetition rate of 2 Hz. The first RF acceleration (from 45 keV to 3 MeV) is done by a 3 m long Radio Frequency Quadrupole. At 3 MeV the beam enters a 3.6 meter long chopper line, consisting of 11 quadrupoles, 3 bunchers and two sets of deflecting plates. The beam is then further accelerated to 50 MeV in a conventional Drift Tube Linac (DTL). The DTL, subdivided in 3 tanks, is 19 meters long. Each of the 111 drift tubes is equipped with a Permanet Magnet Quadrupole (PMQ). The acceleration from 50 to 100 MeV is provided by a Cell-Coupled Drift Tube Linac (CCDTL). The CCDTL is made of 21 tanks of 3 cells each for a total length of 25 meters. Three tanks are powered by the same klystron, and constitute a module. The focusing is provided by electromagnetic quadrupoles placed outside each tank, with the option of using Permanet Magnet Quadrupoles between coupled tanks. The acceleration from 100 to 160 MeV is done in a PI-Mode structure. The PIMS is made of 12 tanks of 7 cells each for a total of 22 m. Focusing is provided by 12 Electromagnetic Quadrupoles (EMQ)

The integrated gradient of the 150 quadrupoles (2/3 of which are permanent quads) and the phase and amplitude of the 260 RF accelerating gaps are shown in Figures 1-3.

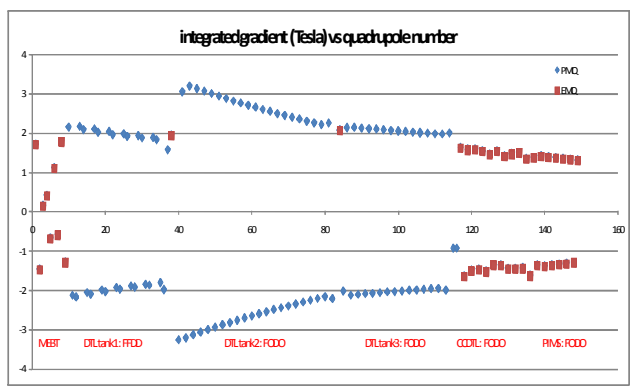

Figure 1: Integrated gradient vs. quadrupole number. Blue diamonds = PMQ; red square = EMQs

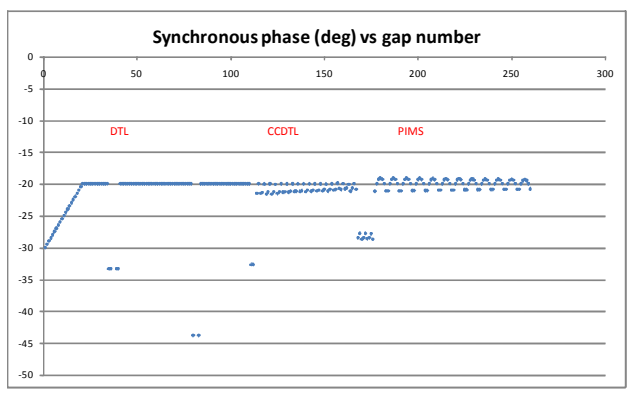

Figure 2: RF Phase vs. gap number.

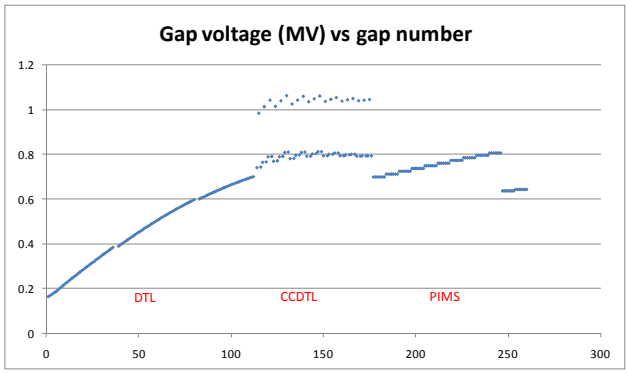

Figure 3: RF Voltage vs. gap number.

Nominal Beam dynamics

The beam dynamics in each of the 4 accelerating structures of Linac4 (RFQ, DTL, CCDTL and PIMS) has been carefully optimised to guarantee the minimum emittance growth together with the maximum transmission. Efforts have been made to control the transverse and longitudinal phase advance in order to avoid resonances and sharp transitions at any time [5]. Efforts have also been made to be able to accept a wide range of beam currents in a focusing system of which 2/3 are permanent magnet quadrupoles. In general the best beam quality is obtained when the focusing is as extended as possible, when drift spaces without active elements are minimised, basically when the time when space charge forces are left unbalanced is reduced to a minimum. This approach, especially at the low energy end, leads to limited space for passive elements like diagnostics that are nevertheless necessary for the good functioning of the machine. The integration of the accelerating structures in a real beam line has caused therefore a general degradation of the emittance accompanied by formation of halo. There are two sections in Linac4 where the most of the emittance increase is localised: the 45 keV LEBT and the 3MeV MEBT housing the chopper line. In the LEBT (1.9 m long) the beam is assumed to be 90% neutralised, therefore the emittance increase is not due to space charge but mostly to the very high divergence (about 200 mrad) with which the beam comes out of the source. Infact such a divergence is almost comparable to the transverse momentum given by the entrance fringe field of the first solenoid, making it impossible to completely cancel out the azimuthal component at the solenoid exit fringe field. Such an effect amounts for 15% emittance increase, but most importantly leads to the distortion of the transverse phase space (see Fig 5) that pushes a few percent of the particles outside the RFQ transverse acceptance.

In order to minimise irradiation at high energy and in general in order to better tailor the 352 MHz time structure of the Linac pulse to the 1 MHz CERN PS Booster bucket a device capable of removing a defined number of micro-bunches from the Linac pulse is housed in the space between the RFQ and the DTL. This device (chopper) [6] provides an electric field perpendicular to the direction of propagation of the beam is applied between two parallel plates. The strict requirement on the rise time (less than 2 ns) limit the maximum applicable voltage to the kV range, therefore forcing to use plates with an active length of the order of one meter to achieve the separation needed to remove the unwanted beam. Such a bulky object cannot be spread over several focusing periods (which would nullify its effect) and therefore the only solution is to increase (in our case by a factor of 10) the length of the focusing period in the transition between the RFQ and the DTL. This is however detrimental to the continuity of the phase advance and to transverse and longitudinal beam emittance conservation, especially in presence of space charge forces. The transverse emittance increase in the MEBT is of the order of 20%, to be compared with an overall emittance increase over the whole Linac4 of about 40%. After 12 MeV there is virtually no emittance increase, within the statistical fluctuations.

Figure 4 shows the rms transverse emittances along Linac4, the transition between structures are indicated with a triangular marker. It is worth noticing that the emittance decrease at z= 8 m , corresponding to the 3MeV off line beam dump, is due to a controlled beam clean up that is supposed to remove the halo particles coming from the source, LEBT and RFQ. The amount of particles removed depends on the optics (between 3 and 12 %) and operational experience with the 3 MeV test stand in 2010 [7] will give us an insight on the benefits of this approach.

Linac4 will start operating as an injector to the PS Booster at a moderate duty cycle (10^{-3}) but it is designed with the potential to become the front-end of a Superconducting Proton Linac operating at a beam duty cycle of up to 6%, therefore the control of the losses and the activation of the machine have been a design criteria build into the basic layout. It has been decided to have a ratio between the rms beam size and the beam vacuum chamber of at least 6, everywhere after the beam reaches 3 MeV of energy, which is considered the threshold for neutron production in copper. Figure 6 shows the ratio between the bore aperture and the RMS beam size in Linac4: the bottlenecks are at low energy, in the LEBT and in the MEBT, whereas from 3 MeV the ratio is always above 6 and from 100 MeV is above 8. In simulations no losses are observed in the LEBT, whereas in the MEBT losses are located on the chopper plates and on the dump. Activation is not an issue at these energies. The nominal transmission from the source to the end of the PIMS is 85%, not including H- stripping losses. The loss pattern is shown in Figure 7. In the next two chapters the special features of Linac4, chopping and energy ramping are described in detail. Both these actions, which are costly in terms of pure Linac beam dynamics, are aimed at better matching longitudinally the Linac beam into a ring.

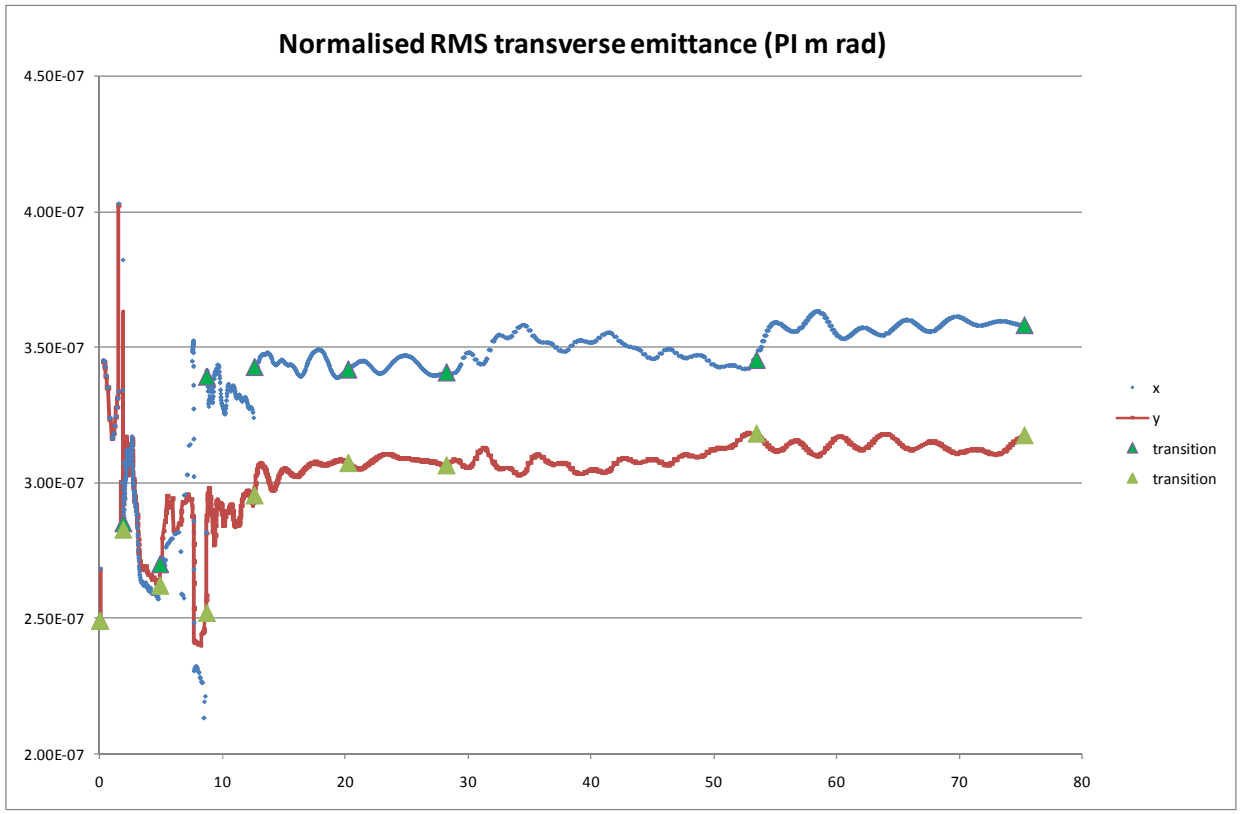

Figure 4: Normalised transverse emittances along Linac4. The triangles indicate the transition between the different structures.

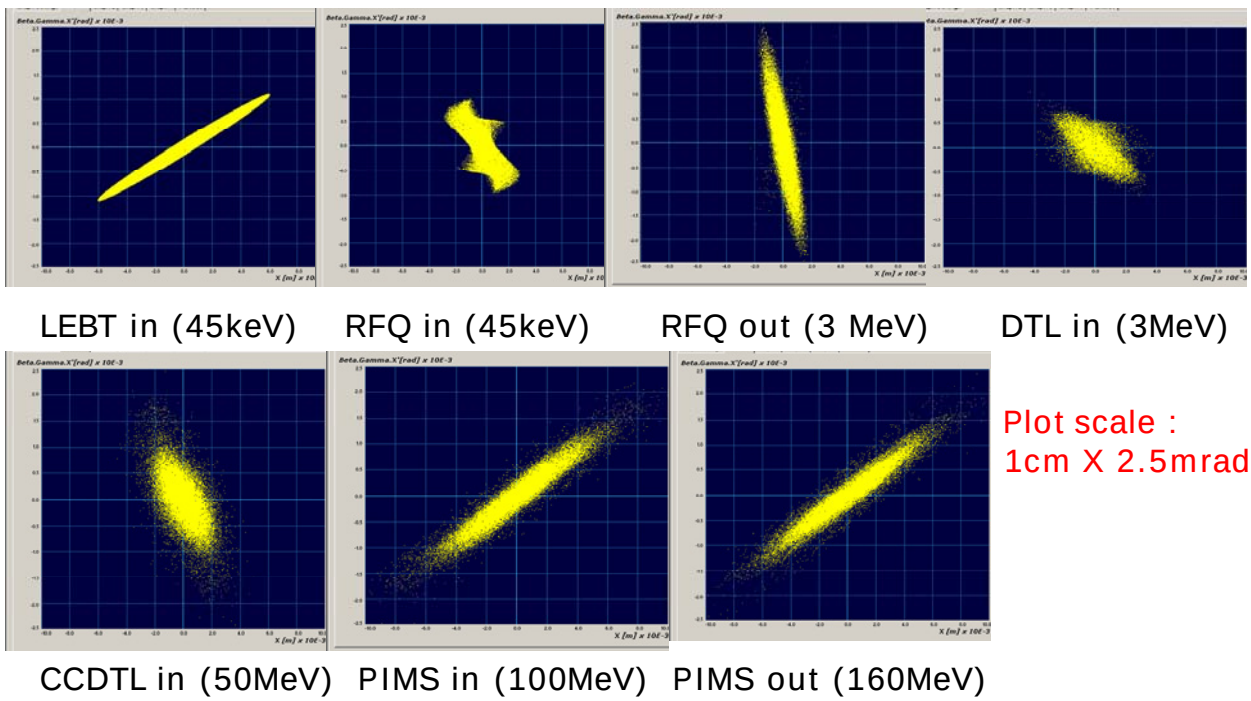

Figure 5: Normalised transverse phase space at the transition between structures in Linac4.

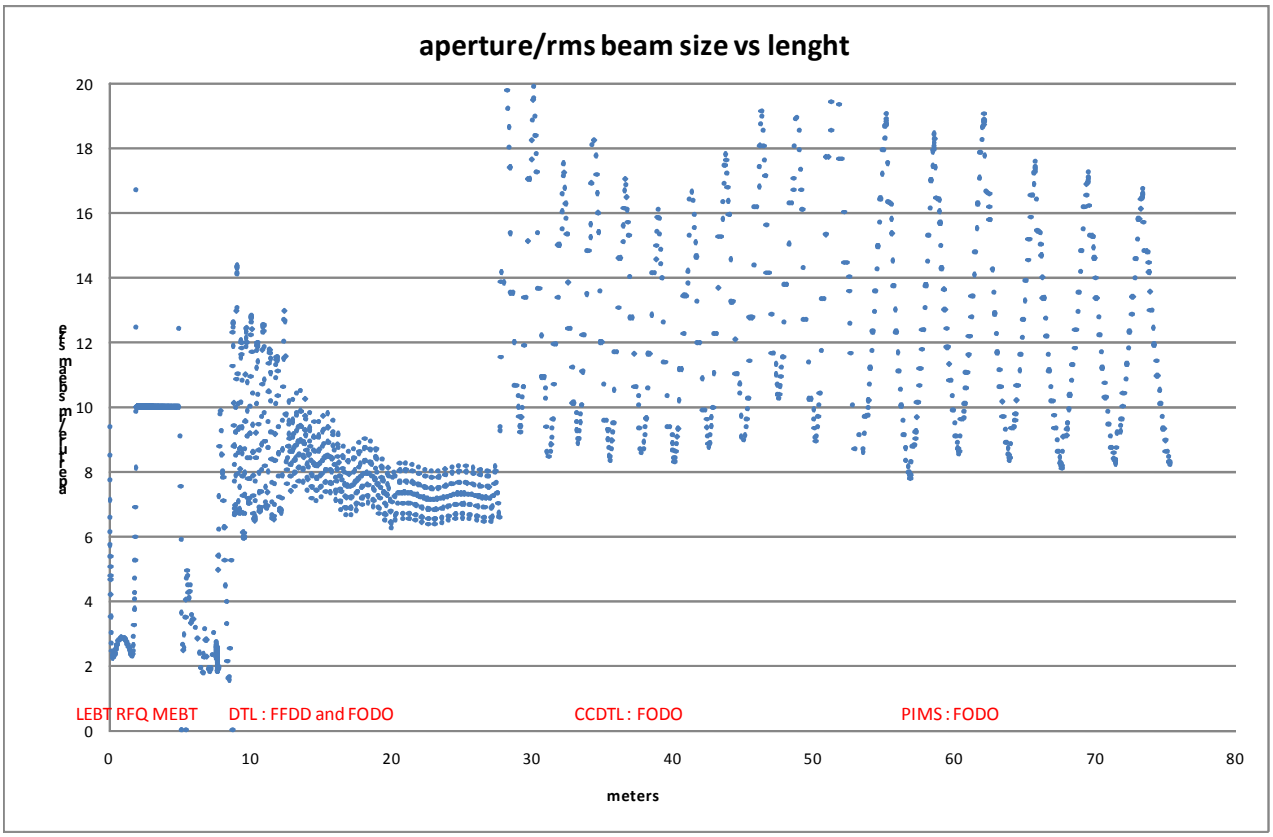

Figure 6: Ratio between the bore aperture and the RMS beam size in Linac4.

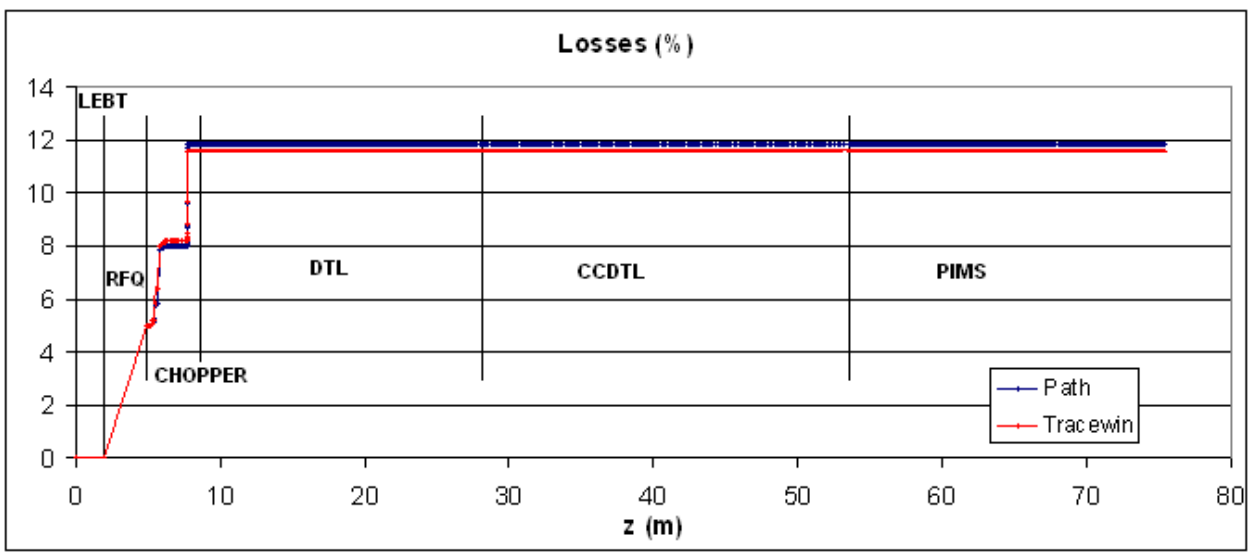

Figure 7: Nominal losses in Linac4, predicted by two different beam dynamics codes.

Chopping

The 3 MeV line between the RFQ and the DTL houses a fast-switching electrostatic device able to remove 150/352 micro-bunches (and ultimately 3/8 micro-bunches) and a conical-shaped dump to dispose of the chopped micro-bunches [7]. The device is embedded in a quadrupole, to limit beam quality deterioration. An effective applied voltage of 500 Volts translates in a kick of 6.6 mrad, which guarantees an almost complete separation of the wanted and unwanted micro-bunches: a mere 0.03% of the chopped beam is not intercepted at the dump and is lost in the DTL. A higher voltage (550Volts) would completely separate the two beams. The transverse phase space in the plane of chopping at the end of the chopper and at the end of the dump are shown in Figure 8(a,b).

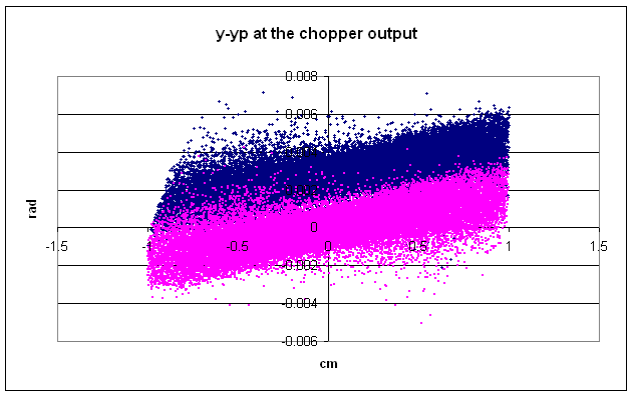

Figure 8(a,b): Chopped and unchopped beam at the end of the chopper (top) and at the end of the dump (bottom).

The chopped beam will be intercepted by a conical shaped dump [7], 120 mm in length and with a minimum radius of 6 mm. The power deposition on the dump is as uniform as possible, in order to minimise the power per unit surface. This is an issue only for the high duty cycle operation as the dump can stand up to 2 MW/m^2. The mark of the chopped beam on the dump can be seen in Figure 9.

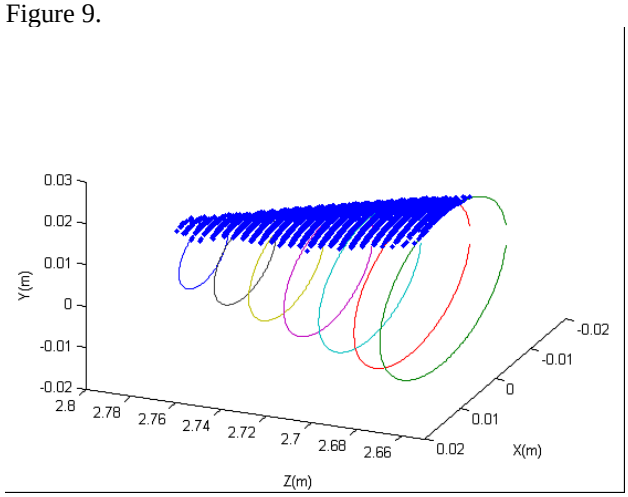

Figure 9: Footprint of the beam on the dump conical surface. The rings indicate the size of the dump cross-session and the dots represent the beam. The beam travels from right to left.

Energy ramping

In order to have a more uniform longitudinal distribution inside the the PS booster bucket, the average energy of the linac is varied over 20 injection turns by 1 MeV (up and down) [8]. In this way the PS booster longitudinal bucket is “painted” as it is shown in the sketch on Figure 10. From the linac dynamics and hardware point of view this operation implies varing linearly (up and down) the field in the last two tanks of the PIMS by 10% over 10 + 10 μs. (20 turns) . In order to ease this task the last two tanks of the PIMS are run at a lower field than the maximum attainable (2.9 instead of 3.8 MV/m). The field distribution in the PIMS tanks is shown in Figure 11 and Figure 12 shows the effect on the longitudinal beam phase space: the beam distribution is unmodified and the average energy is changed by ±1 MeV.

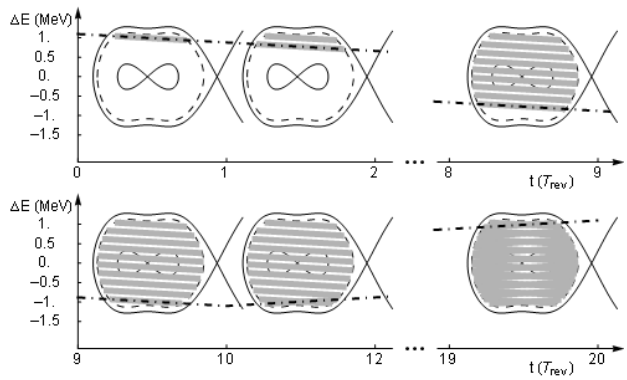

Figure 10: Sketch of the energy painting in the PS booster (courtesy of C. Carli).

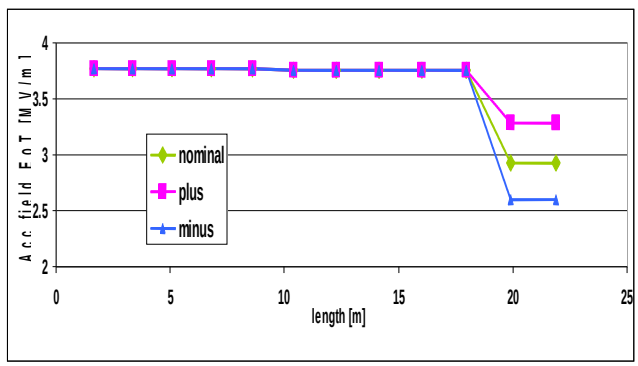

Figure 11: Accelerating field in the PIMS: the last two tanks are varied for energy ramping.

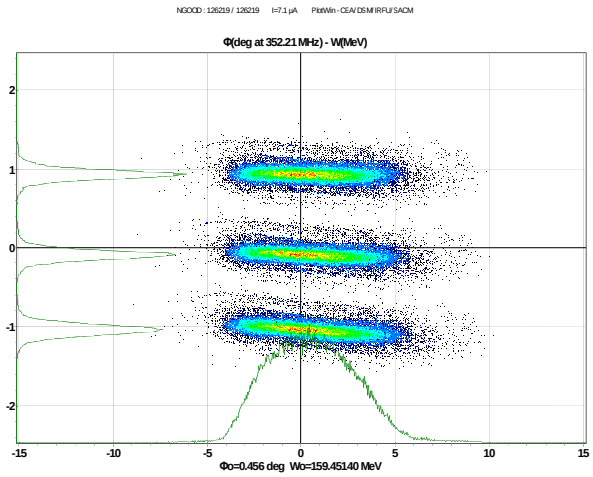

Figure 12: Longitudinal phase space (Energy in MeV vs phase in deg) of the beam with nominal beam energy (centre) and the two extremes of the energy ramping.

ERROR STUDIES

The behaviour of the machine under the influence of beam alignment errors, quadrupole alignment errors, quadrupole gradient errors, beam energy jitters and RF phase and amplitude errors has been evaluated in a dedicated series of statistical runs. For simplicity the errors have been divided into two main categories: transverse and longitudinal. Transverse errors include alignment errors (beam and quadrupoles) and quadrupole gradient errors. Longitudinal errors include beam energy jitter, RF phase and amplitude errors. Typically transverse errors affect transmission , transverse emittance and the orbit of the beam, whereas longitudinal error have an effect on the "effective" transmission, i.e. the percentage of accelerated particles, as well as longitudinal emittance and energy jitter. It has been verified that the effects of transverse and longitudinal errors sum up and that in first approximation there isn't any strong cross-correlation. In the next paragraphs the results of the transverse errors studies and the longitudinal ones will be described in detail.

Transverse error studies-procedure

The purpose of the transverse error studies is three-fold. First of all it aims at probing the stability of the machine under the influence of errors, secondly it aims at defining an alignment tolerance for the focusing elements and finally it aims at defining the number, position and strength of the dipole correctors (steerers) and monitors needed to control the remnant trajectory errors in the machine. The procedure that has been followed is to perform a series of about 2000 runs with PATH or TRACEWIN (which give equivalent results) with different errors settings and to log for each run the beam losses, the emittance growth and the beam trajectory. In this first phase we can observe the sensitivity of the machine, identify the weak spots and the sensitive parameters and possibly make modification to the optics to reduce the sensitivity. Once this first phase is over, the correction system is applied on the worst cases and a steering procedure identical to the one that would be used in the operations of a real accelerator is put in place. An optimising routine cycles over the steerers in order to find the minimum orbit excursion at the position of the monitors, together with the maximum transmission. Often the maximum transmission is not achieved with the minimum orbit excursion, due to the possible misalignment of the focusing elements. The number of steerers and monitors is increased until the maximum average losses are below 1 W/m at 6% beam duty cycle and the transverse additional emittance growth at 2 sigma is limited to 15-20% with respect to the nominal case. These two conditions are dictated by the shielding and by the emittance budget of the PS-Booster.

The results of these studies [9] show that errors as detailed in Table 1 can be compensated by a system composed of 15 independent horizontal and vertical steerers with an integrated field of 3.5 10^{-3} T m and 15 beam position monitors with an accuracy of at least 0.5 mm. An example of beam trajectory in the DTL before and after steering can be seen in Figure 13 and the corresponding transmission in Figure 14.

Table 1: Transverse errors

Error	Amplitude	Distribution
Quadrupole transverse position	±0.1 mm 1sigma	Gaussian
Quadrupole angles (3)	±1 mrad 1sigma	Gaussian
Quadrupole gradient	±0.5% total	Uniform
Beam transverse position	±0.3 mm 1sigma	Gaussian
Beam angles	±0.3 mrad 1sigma	Gaussian

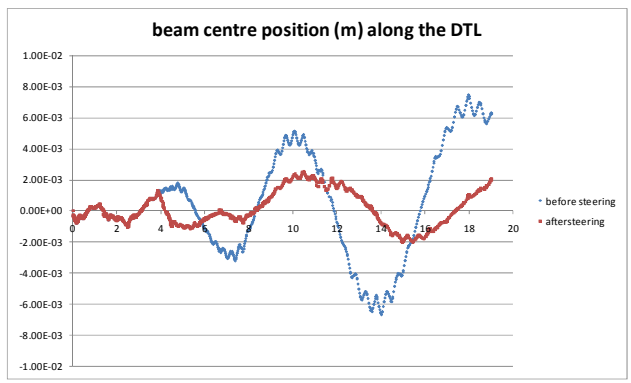

Figure 13: Beam centre position under the effect of one possible set of transverse errors before and after steering in the DTL.

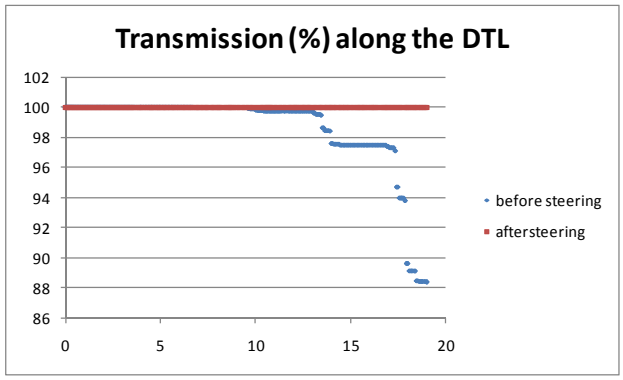

Figure 14: Transmission under the effect of one possible set of transverse errors before and after steering in the DTL.

Transverse error studies-loss map

A side product of the several thousand runs with different error distribution is a comprehensive map of the losses along the linac. In all the runs the location and energy of the particle lost has been recorded and the maximum losses have been calculated at the highest foreseeable beam duty cycle, i.e. 6%. The loss map has been used as input for radioprotection calculation and it demonstrates that the Linac4, also at high duty cycle, is radiologically safe as the losses can be controlled to 1W/m. The hottest point in the machine is at the transition between the CCDTL and the PIMS. In order to achieve the required power loss accuracy the beam has been represented by 500 000 macro-particles (Figure 15).

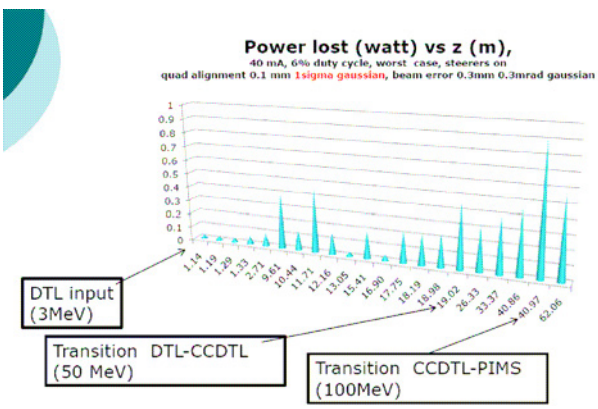

Figure 15: Loss map of Linac4, starting from the DTL input (3 MeV).

Longitudinal error studies

The longitudinal errors that we have considered in the studies are of two types: the “dynamic” or klystron errors and the “static” or gap errors. Klystron phase and amplitude errors come from a real jitter in the amplitude and phase of the RF power source. The timescale of this jitter is not known at the moment, whether it varies bunch-to-bunch or it has a longer timescale. The klystron errors affect mostly the output beam energy and phase jitter. They are correlated over many gaps (all the gaps powered by the same klystron, up to 40 in Linac4) and cannot be cured.

Gap amplitude errors are due to tuning and/or manufacturing imperfection, they are static and they affect mostly the longitudinal emittance. They are uncorrelated between one gap and the next one or, if they are, their average is zero over several gaps. Their effect can be generally mitigated by increasing the RF power above nominal.

For klystron errors we have considered values between ±0.5% and ±2% for the amplitude and values between 0.5 and 2 degrees for the phase. We have also introduced an uniform input energy jitter coming from the previous stage of acceleration, which we estimate at 6KeV at the input of the DTL, 90 keV at the input of the CCDTL and 250 keV at the input of the PIMS. Those values turned out to be coherent with the results of the error studies.

In Table 2 we report in detail the results of the effect of a klystron error on the beam phase and energy jitter and r.m.s. emittance at the end of the DTL. From the results we can deduce that the amplitude error has more effect than the phase errors and that a variation of ±2% in amplitude causes an emittance growth and an energy jitter above what is acceptable. A control of the amplitude and phase within ± 0.5% and ±0.5 degrees would be ideal but a control within ±1% and ±1 degree is also acceptable.

Table 2: Effects of Klystron errors in the DTL

Klystron amplitude and phase errors	Phase jitter [deg] 1sigma	Energy jitter [keV] 1sigma	RMS Emittance [deg MeV]
nominal			0.167
0.5% and 0.5 deg	0.8	13	0.169±0.003
0.5% and 1 deg	0.9	18	0.171±0.004
0.5% and 2 deg	1.1	31	0.175±0.009
1% and 0.5 deg	1.6	23	0.1707±0.005
1% and 1 deg	1.6	28	0.1719±0.006
1% and 2 deg	1.8	36	0.1772±0.011
2% and 0.5 deg	5.1	43	0.179±0.014
2% and 1 deg	5.7	46	0.180±0.017
2% and 2 deg	8.6	49	0.187±0.024

Equivalent runs have been done for the CCDTL and the PIMS (Tables 3 and 4) and the results confirm that Klystron phase and amplitude should be controlled ideally to 0.5% 0.5 deg to control energy and phase jitter at the CCDTL and PIMS output but that a value of 1% and 1deg are still acceptable. For the PIMS the value of 1% and 1 degrees is an hard limit, as the maximum energy jitter acceptable for a successful energy painting is 125keV (1sigma value).

Table 3: Effects of Klystron errors in the CCDTL

Klystron amplitude and phase errors	Phase jitter [deg] 1sigma	Energy jitter [keV] 1sigma	RMS Emittance [deg MeV]
nominal			0.196
0.5% and 0.5 deg	0.5	39	0.196±0.003
1% and 1 deg	1	63	0.196±0.005
2% and 2 deg	2	115	0.198±0.009
5% and 2 deg	4	237	0.200±0.015

Table 4: Effects of Klystron errors in the PIMS

Klystron amplitude and phase errors	Phase jitter [deg] 1sigma	Energy jitter [keV] 1sigma	RMS Emittance [deg MeV]
nominal			0.180
0.3% and 0.3 deg	0.3	65	0.181±0.00088
0.5% and 0.5 deg	0.4	78	0.181±0.00094
1% and 1 deg	0.66	126	0.181±0.0012
2% and 1 deg	0.85	220	0.181±0.0013

The effects of the "static" errors were evaluated independently of the effects of the "dynamic" errors. In the 3 DTL tanks gap amplitude errors were assigned randomly and independently to the 111 gaps with an uniform distribution over ±1% to ±10% of the nominal voltage of each gap. In the CCDTL a tilt inside each tank, correlated over the module was applied with amplitudes varying from ±1% to ±5%. In the PIMS two types of error distribution were applied: a tilt over each tanks as well as an elliptical distribution with variations from ±1% to ±10%. In all cases the average of the individual errors has been readjusted to be equal to the nominal value, which in practical terms is equivalent to adjusting the RF power in each tank to achieve the nominal average field.

In all cases we found that the structures of Linac4 are quite insensitive to static errors, and that amplitude of 2% in DTL and CCDTL and tilt of up to 5% in PIMS can be tolerated by adjusting the average field to the nominal value

An example of the field error distribution applied in the case of linear and elliptical tilt in the PIMS is shown in Figure 16(a,b). All the results of the simulation are reported in [10].

Beam losses were never observed in any of the cases analysed.

CONCLUSION

The beam dynamics studies of Linac4 with the codes TRACEWIN and PATH show that the layout, the focusing and the correction system adopted should allow the production of a high quality beam both for the present CERN PS Booster injection as well as for a future Superconducting Proton Linac. Moreover transverse alignment tolerances and a correction system have been defined to allow safe operation up to a duty cycle of 6%.

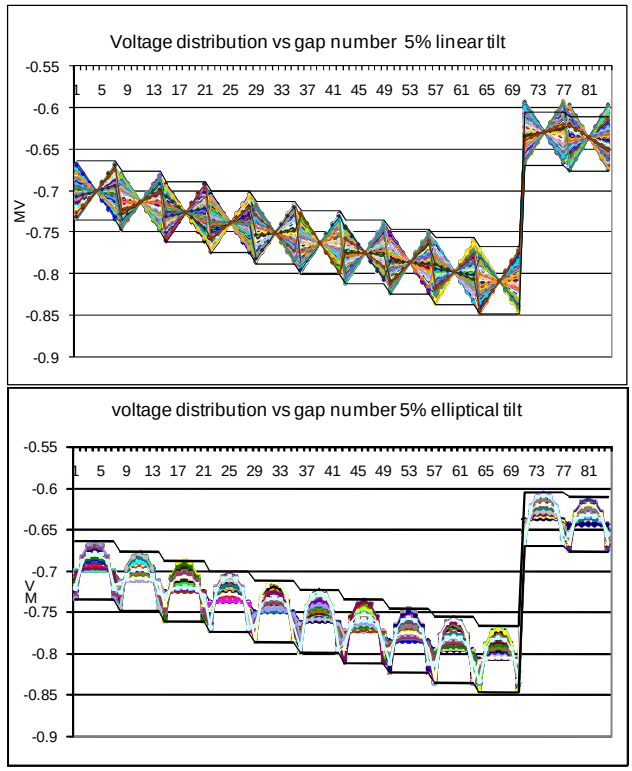

Figure 16(a,b): Static voltage error distribution in the PIMS for 5% linear tilt (top) an 5% elliptical tilt (bottom) the black lines indicate the 5% limit and the average correspond to the nominal value.

The effects of RF errors on the beam quality have been evaluated and limit for klystrons and gap errors have been defined.

REFERENCES

[1] M. Vretenar ed., LINAC4 technical Design Report, CERN-AB-2006-084 ABP/RF (2006).
[2] F. Gerigk ed., SPL Conceptual Design Report CERN-2006-006 (2006).
[3] A. Perrin, J.F. Amand, Travel User Manual (2003).
[4] R. Duperrier, N. Pichoff, D. Uriot, ICCS 2002 Proceedings.
[5] I. Hofmann et al., "Review of beam dynamics and space charge resonances in high intensity linacs", EPAC'02 proceedings, Paris, France (2002).
[6] M. Paoluzzi et al., CERN-AB-Note-2008-040 (2008). F. Caspers et al., "The CERN-SPL Chopper Concept and Final Layout", EPAC'04 Proceedings (2004).
[7] J-B. Lallement et al., "Measurement strategy for the CERN Linac4 chopper line", HB2006 Proceedings, Tsukuba, Japan (2006).
[8] M. Aiba et al, TUPAN093, PAC'07, NM, USA, 2007. C. Carli, R. Garoby CERN-AB-Note-2008-011 (2008).
[9] A.M.Lombardi et al, CERN-AB-Note-2007-033 (2007).
[10] Note in writing.